doi: 10.5028/jatm.v8i3.643

Shear Properties of Carbon Fiber/Phenolic Resin Composites Heat Treated at High Temperatures

Homero Paula Silva[1], Luiz Cláudio Pardini[2], Edison Bittencourt[3]

ABSTRACT: Carbon fiber/phenolic resin composites have long been used as ablative materials in rocketry. Ablation is a complex multiscale problem where radiative and convective heating leads to the pyrolysis of phenolic resin matrix, resulting in the formation of a porous insulation char as thermal protection. This study investigates the shear properties evolution during the heat treatment of a carbon fiber/phenolic resin nozzle extension entrance (exit cone) which is part of an integrated nozzle of launching and sounding vehicles, developed at the Instituto de Aeronáutica e Espaço (SP), Brazil. Specimens of the material (carbon fiber/phenolic resin composite) were subjected to heat treatment at 500, 1,000, 1,500 and 2,000°C, and measurements of shear strength and shear modulus were performed using the Iosipescu mode. Experimental data were compared with the results obtained theoretically. Also, morphological analysis was accomplished by optical microscopy and the observation of fractured surfaces, by scanning electron microscopy. Significant morphological changes in the microstructure after heat treatments were observed. The lowest value for shear strength obtained experimentally was 4.05 MPa, which is greater than the ultimate value obtained analytically (2.35 MPa), fulfilling its structural function during the propulsion time.

KEYWORDS: Ablation, Carbon-phenolic, Shear strength.

INTRODUCTION

The state-of-the-art thermal protection systems are based either on ablative or reusable material depending mainly on the mission and trajectory characteristics. These include mainly bulk carbon, ceramics, carbon/ceramic composites and ceramic matrix composites eventually coated with refractory materials such as HfC, ZrC, and SiC. Also ablative systems based on organic polymer matrices are used as thermal protection structures (Almeida 2007; Tick *et al.* 1965).

The launching and sounding vehicles are important devices for research and practical and commercial use of space. They represent the transport system by which satellites, human beings and inhabited stations are placed into Earth's orbit. Additionally, microgravity experiments are conducted inside and outside the Earth's atmosphere and missions to space exploration (Gonçalves 2008). In all the space vehicles used as space devices a thermal protection system is needed in order to protect the structure systems, as well as the electrical system and the payload (Dias 2001).

Many components and integrated systems of launching vehicles are manufactured in composites in order to meet 2 basic design requirements for space vehicles that are stiffness and mechanical strength combined with low weight and heat resistance (Savage 1993). Besides, mass reduction for components such as fairing, fins and motor cases is critical since they represent an increase in payload (Barbosa 2004; Martins 2014).

The landmark of thermal protection systems used in rocketry are based on carbon fiber/phenolic resin composites due to their exceptional ablative properties, light weight and adequate

1.Departamento de Ciência e Tecnologia Aeroespacial – Instituto de Aeronáutica e Espaço – Divisão de Mecânica – São José dos Campos/SP – Brazil. **2.**Departamento de Ciência e Tecnologia Aeroespacial – Instituto de Aeronáutica e Espaço – Divisão de Materiais – São José dos Campos/SP – Brazil. **3.**Universidade Estadual de Campinas – Faculdade de Engenharia Química – Departamento de Tecnologia de Polímeros – Campinas/SP – Brazil.

Author for correspondence: Homero Paula Silva | Departamento de Ciência e Tecnologia Aeroespacial – Instituto de Aeronáutica e Espaço – Divisão de Mecânica | Praça Marechal Eduardo Gomes, 50 – Vila das Acácias | CEP: 12.228-904 – São José dos Campos/SP – Brazil | Email: homerohps@iae.cta.br

Received: 03/18/2016 | **Accepted:** 05/31/2016

strength after char formation (Williams and Cury 1992; Nichols and Hall 1988a,b; Hall 1988a,b). Some of these items made of composites for launching vehicles are exposed during a certain period of time under extreme temperature excursions (above 1,000 °C) and to high-speed gas flow (Mach 3), as is the case of the nozzle extension (exit cone), shown in Fig. 1. The exit cone is the region of the nozzle where gas flows from the propellant burning. Usually, these parts are exposed to temperatures from 2,000 to 3,000 °C, which exceeds by far the working service limit of conventional alloys (Silva 2015).

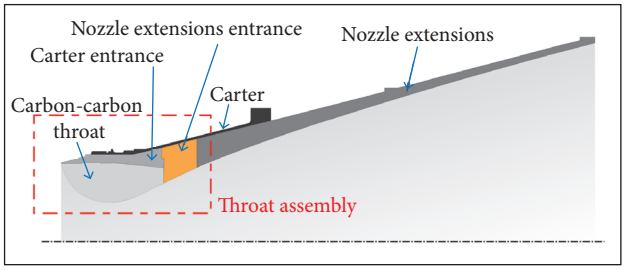

Figure 1. Nozzle and throat assembly in detail.

The heat absorbed by the composite structure (carbon fiber/phenolic resin) causes endothermic processes because the area in contact with the gas flow undergoes a pyrolysis process. To this phenomenon is given the name of ablation (Barbosa 2004; Minges 1969).

The composites used as thermal protection systems have to present high heat capacity to dissipate heat per unit mass (Nichols and Hall 1988a,b; Barbosa 2004). Among the composites that meet these requirements carbon fiber/phenolic resin (CFPR) composites play a major role (Pardini and Levy Neto 2006; Thimoteo 1986). The choice of phenolic resin as matrix structure is because it has high carbon yield content when subjected to pyrolysis. The porous carbon residue structure obtained during the ablation process is a result of absorbed heat and protects the structural elements (Silva 2015).

Typical ablative materials properties, based on phenolic resin/carbon fiber, phenolic resin/silica fiber and polyamide/phenolic composites are shown in Table 1. The table shows that low density and significant insulation properties are displayed by the polyamide/phenolic composite, while outstanding ablative efficiency is presented by the carbon fiber/phenolic composite.

In a typical design of rocket nozzles, different components and parts having specific functions constitute the "throat assembly", namely, carter entrance, nozzle extension entrance and throat, as shown schematically in Fig. 1.

All these mechanical parts are fit and assembled together by structural bonding. The carter entrance and nozzle extension entrance are manufactured of a carbon fiber/phenolic resin composite by hot-pressing process. The main throat region is made of carbon fiber reinforced carbon composite. During the burning time, wear produced by the gas flow associated with the heat generation and propagation through the structure (ablation phenomena) in the nozzle extension entrance affects mechanical and thermal properties weakening the overall attachment area. This can result in throat expulsion resulting in mission failure.

This study aims to evaluate the loss of shear strength of carbon fiber/phenolic composites extracted from nozzle extension entrance material as a function of heat treatment temperature. The reduction in shear properties is critical since composites are laminar and prone to failure by delamination. Also the resulting morphological changes were observed by optical microscopy and scanning electron microscopy (SEM).

EXPERIMENTAL

MATERIALS

Composites were made at Plastflow Ltda. The carbon fiber fabric used is rayon based, T22R-ECHO, having a fiber density of 1.55 g·cm^{-3}. The fabric has a thickness of 0.45 mm, weave

Table 1. Protective efficiency of representative composite ablators.

Composite	Density (g·cm^{-3})	Ablative efficiency[a] (MJ·kg^{-1})	Insulation index[b] (s)
Carbon fiber fabric (65%/weight) / phenolic resin (35%/weight)	1.39	160[c]	30
Silica fiber fabric (65%/weight) / phenolic resin (35%/weight)	1.55	27[c]	65
Polyamide (50%/weight powder)/phenolic resin (25%/weight)/25% (phenolic microballons)	0.59	35[d]	258

[a]Heat of ablation; [b]Time for back wall to reach 150 °C ; [c]Stagnation enthalpy = 21.6 MJ·kg^{-1}; [d]Stagnation enthalpy = 18.6 MJ·kg^{-1}. Source: Neuse (1973).

pattern of 2 × 2 Twill, and areal weight of 350 ± 35 g·m^{-2}. A phenolic resin resol type matrix with a viscosity of 1,000 cPs at 20 °C has been used. The "prepregging" process was carried out at the Plastflow facilities. After wetting, the percentage fiber weight reached 55 – 60%.

METHODOLOGY

The prepregged fabrics were cut in the form of "petals" and arranged on the base of a ring-shape metallic mold so that the splices are lagged during stacking of the layers, as shown schematically in Fig. 2.

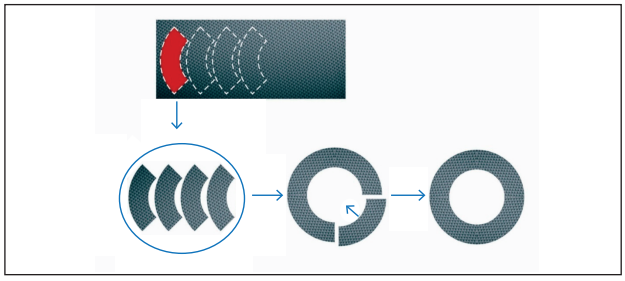

Figure 2. Scheme of carbon fiber "prepregged petals" arranged in the ring shape for lay-up molding.

The mold is then closed and the material (carbon fiber impregnated with phenolic resin) is cured by hot molding process, using a hydraulic press with a capacity of 200 tons provided with 2 platforms heated by means of electric resistors, coupled to 2 temperature controllers (a controller for each platform). The cure cycle is 2 h at 100 °C, 2 h at 120 °C, 2 h at 140 °C and 30 h at 165 °C under a pressure of 7 MPa. The material is released from the mold and the rough geometry is called "blank".

The test specimens were extracted from the nozzle extension entrance. Twenty-five specimens were trimmed from the "blank" piece, as shown schematically in Fig. 3, to approximate dimensions of 22 mm (height), 77 mm (length), and 4 mm (thickness). Samples were taken in radial direction from the inner surface of the blank piece, as shown in Fig. 3. In this way, the test coupon comprises stacked carbon fiber fabric layers. Samples were subjected to heat treatments (500, 1,000, 1,500 and 2,000 °C) in an electric furnace under inert nitrogen atmosphere. Heat treatment gradually converts the phenolic resin matrix to a carbon matrix completely at 1,000 °C.

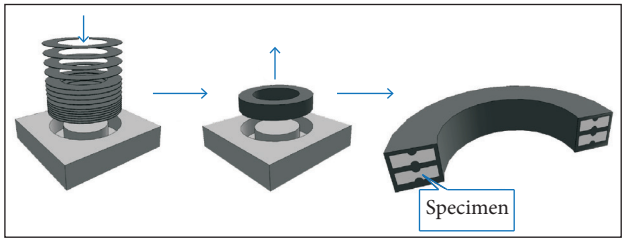

Figure 3. Scheme from molding the nozzle extension entrance blank and cutting the Iosipescu specimens.

Five specimens were tested for each temperature level. The specimens (S) were identified according to the respective temperature level, as-moulded, S500, S1000, S1500 and S2000. The heating rate used was 2 °C·min^{-1} up and hold for 1 min at each temperature. The mass loss was monitored by weighting the sample before and after heat treatment, using a precision scale METLER® PB 8001 model.

The specimens have been finally machined in the dimensions according to ASTM D5379/A 5379M-93. The test fixture and the strain gages positions attached to the samples for measuring shear strain are shown in Fig. 4.

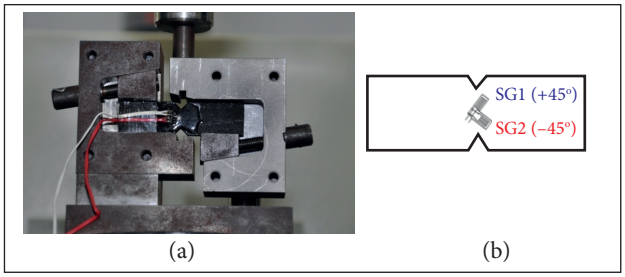

Figure 4. (a) Iosipescu fixture and sample attached to it for testing; (b) Positioning of strain gages in the sample geometry.

The standard ASTM D5379/A 5379M-93 defines the Iosipescu shear strength, calculated according to the equation:

$$\tau = \frac{P\max}{l.e} \quad (1)$$

where: τ is the ultimate shear stress, in MPa; P_{max} is the maximum load failure, in N; l represents the width of the specimen between the roots of slots, in mm; e is the thickness of the specimen, in mm.

The shear modulus (G_{12}) was calculated from the stress/strain curves, and the strains were measured using strain gages positioned at the central region of the specimens, as shown in Fig. 4b. It can be calculated according with the equation (ASTM D5379/A 5379M-93):

$$G_{12} = \frac{\Delta\tau}{\Delta Y} \quad (2)$$

where: G_{12} is the shear modulus of elasticity, in GPa; $\Delta\tau$ is

the range of shear stress between 2 predetermined points in MPa; ΔY is the strain range between 2 predetermined points, in $\mu m \cdot m^{-1}$.

The correspondent strain to stress value in a predetermined point (i) is given by the sum of the strain in modulus recorded by the strain gages. In this case,

$$Y_i = \left| SG1_i\,(+45°) \right| + \left| SG2_i\,(-45°) \right| \quad (3)$$

where: Y_i is the shear strain at data point i; $SG1_i\,(+45°)$ represents the strain measurement in the +45° positioned strain gage at the point i; $SG2_i\,(-45°)$ represents the strain measurement in the −45° positioned strain gage at the point i.

The tests were carried out in a universal testing machine ZWICK 1474 model with a load cell of 2,500 kg coupled to a computer which graphically process the stress/strain curves. The test speed was 2 $mm \cdot min^{-1}$.

The unheated samples and the thermally treated ones were analyzed by the Zeiss Axio Imager A2m optical microscopy. Cross-sections of these samples were prepared according to standard polishing procedures. The evaluation of the porosity was performed by using the Image J software. The image processing consisted of the following steps: (1) adjusting the contrast; (2) conversion to 256 shades of gray; (3) adjustment "threshold"; (4) measurement of the pore volume. This technique consists in converting the image obtained in 256 levels of gray and to determined value chosen, converts the tones below this value in black and above this value in white (Von Dollinger *et al.* 2014). SEM was carried out in a Zeiss Leo 435VPi.

Analysis of thermal and mechanical stresses caused by temperature excursion along with the pressure exerted by the gas flow during burning time has been presented by Teixeira *et al.* (2007). The mechanical stresses analyzed were tensile and compressive. In this study, the same model was used to evaluate the shear stresses under the same conditions considered in the previous research. The input data for this analysis were taken from carbon fiber/phenolic properties as a function of temperature (Ramesh Kumar *et al.* 2005), as shown in Fig. 5. An axisymmetric model has been used, which gives the distribution of temperatures and stress. Two-dimensional plane elements with 2 degrees of freedom per node for structural analysis (PLANED2D) to 3,056 nodes and 3,033 elements have been considered.

The physical properties used in the analysis were the maximum value obtained in the extreme conditions during burning time (t = 60 s) of a typical nozzle element used in solid rocket motor of brazilian lauchers (Machado 1990).

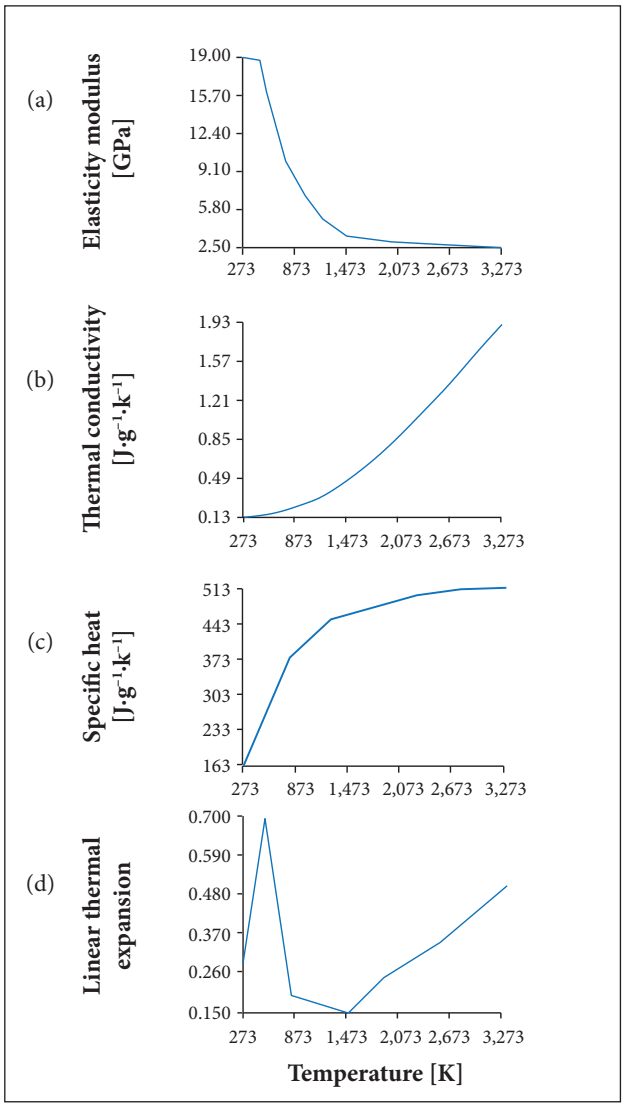

Figure 5. Carbon/phenolic properties as a function of the temperature. (Ramesh Kumar *et al.* 2005).

RESULTS AND DISCUSSION

Table 2 shows the weight loss percentage for the specimens as a function of the heat treatment temperature. Until 1,000 °C the composite mass loss increases as the heat treatment temperature rises, due to pyrolysis of the phenolic resin. Above 1,000 °C, there was no significant increase in mass loss because all phenolic resin of the composite has been carbonized, occurring only oxidation of the carbon fibers.

Table 2. Weight loss of the specimens as a function of heat treatment temperature for the carbon fiber/phenolic resin composite.

Samples	Weight before HT (g)	Weight after HT (g)	Weight loss (%)
As-molded	8.28 ± 0.25	8.28 ± 0.25	0
S500	9.30 ± 0.10	7.64 ± 0.32	8.21 ± 0.28
S1000	9.20 ± 0.30	7.14 ± 0.16	7.76 ± 0.24
S1500	9.10 ± 0.05	6.88 ± 0.02	7.56 ± 0.03
S2000	9.22 ± 0.18	6.84 ± 0.16	7.41 ± 0.16

HT: Heat treatment.

The results of the Iosipescu shear strength and shear modulus tests for the composite samples are shown in Table 3. The results show that a reduction in shear strength occurs as heat temperature goes up to 2,000 °C. Significant reduction in shear strength is noted after 1,000 °C heat treatment. Shear modulus, contrarily, increases as heat treatment temperature goes up to 2,000 °C. These changes are due to progressive pyrolysis of phenolic resin turning on glassy carbon. Heat treatment creates a porous composite microstructure, lowering the strength, but increasing twofold the shear modulus due to the formation of stiffer carbon matrix compared with phenolic resin.

Figures 6 to 10 present the strain measurements during the Iosipescu shear test, as a function of the applied stress. Figure 6a shows the profile of strain behavior during Iosipescu shear test. Figure 6b shows the curves of shear stress as a function of the total strain ($Y_i = |SG1_i(+45°)| + |SG2_i(-45°)|$ for the as-molded carbon fiber/phenolic resin composite. A characteristic non-linearity profile of the stress/strain curve is observed.

Figure 7a shows the strain as a function of shear stress for composites heat treat at 500 °C. The stress/strain curve shown in Fig. 7b has a similar profile to the carbon fiber/phenolic resin composite, where a non-linearity between stress and strain is noticed. However, the strain at failure for the sample heat treated at 500 °C (~ 1.4%) is much lower than the carbon fiber/phenolic resin composite (~ 2.4%). A 15%-reduction in the shear stress is found for sample heat treated at 500 °C, in relation to the pristine composite.

Figure 8a shows the strains as a function of shear stress for composites heat treated at 1,000 °C. It can be seen in Fig. 8b a quasi-linear behavior of the stress/strain curve, unlike to the previous cases. The strain levels are much lower than the as-molded sample (carbon fiber/phenolic resin composite), whereas the strain gages registered a value on the order of 2,000 μm·m^{-1}, i.e. equivalent to about 10% of deformation of the untreated sample. The ultimate shear stress showed a significant decrease, the result obtained is about 18% from shear stress untreated samples value, indicating the weakening of the material to 1,000 °C.

Figure 9a shows the shear strain as a function of shear stress and the shear stress as a function of shear strain for samples subjected to 1,500 °C treatment temperature. It can be seen in Fig. 9b a quasi-linear profile of the curve, similar

Table 3. Ultimate shear strength and shear modulus.

Sample	Ultimate shear strength (MPa)	Shear modulus (GPa)
As-molded	22.5 ± 4.0	1.55 ± 0.6
S500	19.0 ± 2.7	2.69 ± 0.7
S1000	4.0 ± 0.6	3.10 ± 0.3
S1500	4.76 ± 0.3	3.85 ± 0.7
S2000	5.08 ± 0.8	2.90 ± 0.4

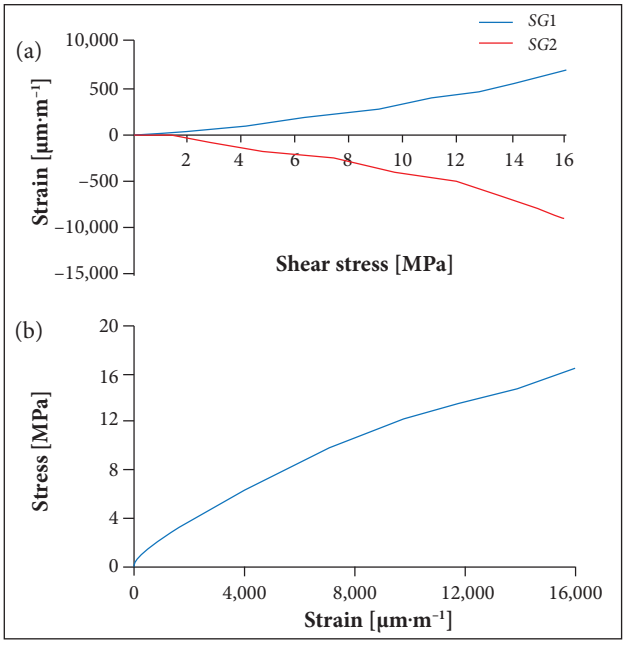

Figure 6. Shear properties for the as-molded carbon fiber/phenolic resin composites under Iosipescu loading mode.

to the previous case. The shear behavior of composites heat treated at 1,500 °C is similar to the composites heat treated at 1,000 °C.

Figure 10a shows strain as a function of applied stress for the composite sample heat treated at 2,000 °C. The strain level obtained for the composite heat treated at 2,000 °C (Fig. 10b) is

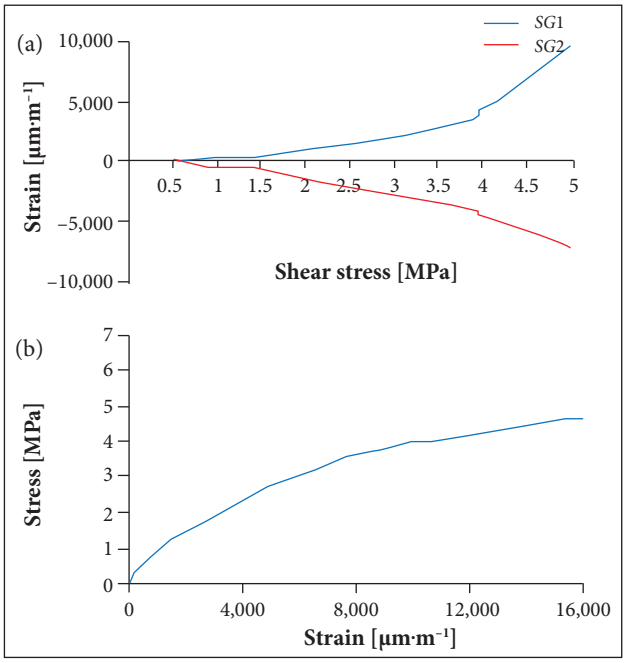

Figure 7. Shear properties for carbon fiber/phenolic resin composites under losipescu loading mode, when heat treated at 500 °C.

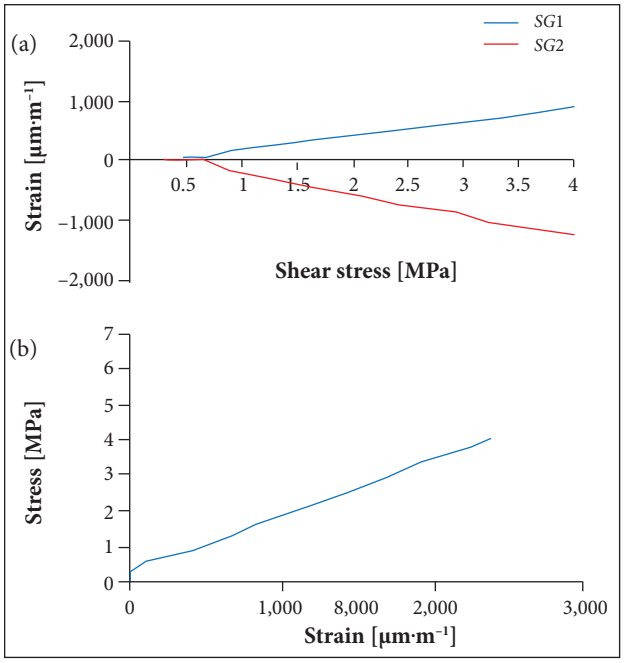

Figure 8. Shear properties for carbon fiber/phenolic resin composites under losipescu loading mode, when heat treated at 1,000 °C.

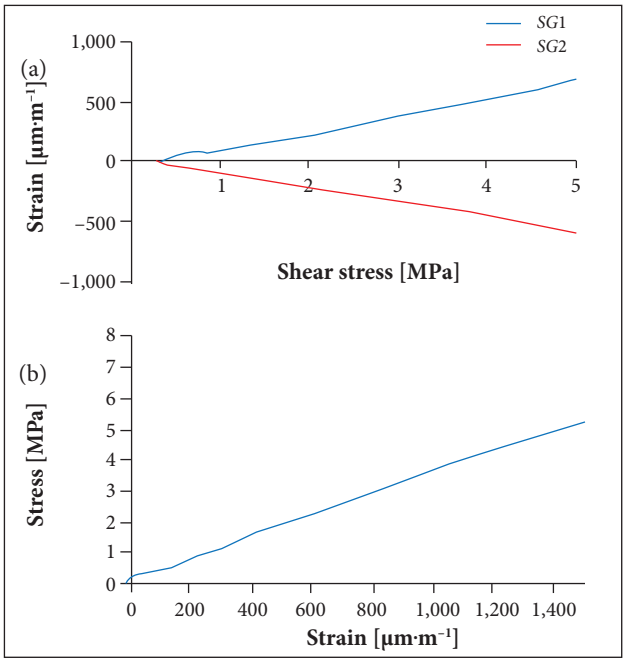

Figure 9. Shear properties for carbon fiber/phenolic resin composites under losipescu loading mode, when heat treated at 1,500 °C.

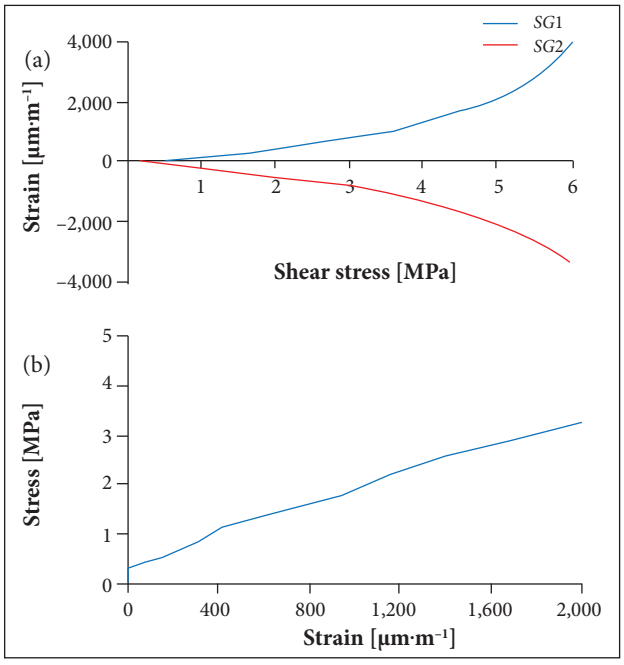

Figure 10. Shear properties for carbon fiber/phenolic resin composites under losipescu loading mode, when heat treated at 2,000 °C.

very similar to the composites heat treated at 1,000 and 1,500 °C. However, strain for the samples heat treated at 2,000 °C is lower than the ones found for 1,000 and 1,500 °C treatments, respectively. For heat treatments beyond 1,700 °C incipient forms of crystalline domains having defined linear edges appear and favors slipping between basal planes when stress is applied, increasing the strain levels (Barbosa 2004).

Figures 11 to 15 show photomicrographs of the pristine composite samples. In Fig. 11, micrographs of the 2 different regions and amplitudes from the carbon fiber/phenolic resin composite, a cross section of the carbon filaments can be identified (position A), and fiber strands in the direction parallel to the picture plane (position B). The distribution of reinforcement fiber strands is not uniform and there are some regions rich in resin as well as pores and microcracks (indicated by red arrows) in between the fiber tows. The positioning of the fiber strands in multiple directions can further enhance strain under shear deformation.

Figure 12 shows, in 2 different regions and amplitudes, photomicrographs of 500 °C treated samples. It is possible to observe matrix-rich regions (C position) and fiber-rich regions (D position). A clear debonded region in the matrix is also found, near to the fiber tows (indicated by red arrows). Debonding is probably due to the contraction process, resulting from the pyrolysis process. Large microcracks are observed in the matrix region, which can be outcome from the shrinkage process during curing or even due to the poor bonding between carbon fiber and phenolic resin. The weave patterns of the fabric layers are not clearly defined.

The heat treatment at 1,000 °C reveals in 2 photomicrographs taken from different regions and amplitudes in Fig. 13 large pores in the matrix regions (indicated by red arrows), which probably arose during pyrolysis as a result of the composite shrinkage. Similarly to Fig. 12, the fiber weave array is not uniform. At this level of heat treatment (1,000 °C) the composite seems to have a large amount of damage caused by the pyrolysis process.

In the photomicrographs of 1,500 °C heat treated samples, Fig. 14 shows, in 2 different regions and amplitude, large fiber agglomerates and few resin-rich regions are seen. It is also observed microcracks throughout the composite cross section, due to composite shrinkage and weight loss during pyrolysis process (indicated by red arrows).

Similarly to 1,500 °C treated samples, Fig. 15, referring to 2,000 °C treated specimens, observed in different regions and amplitudes, also displays few resin-rich regions and many microcracks caused by pyrolysis process (as indicated by red arrows). Significant amount of intra-bundle cracked regions can be seen. The formation of cracks and pores is a characteristic feature of progressive heat treatment process for carbon fiber/phenolic resin composites. Crack and pore formation depends on the type of carbon fiber used for manufacturing the composites. Carbon fiber bonding to the matrix seems to have a significant effect on fiber/matrix and fiber tow/matrix debonding either on the molding stage as well as during the excursion of heat treatment temperature.

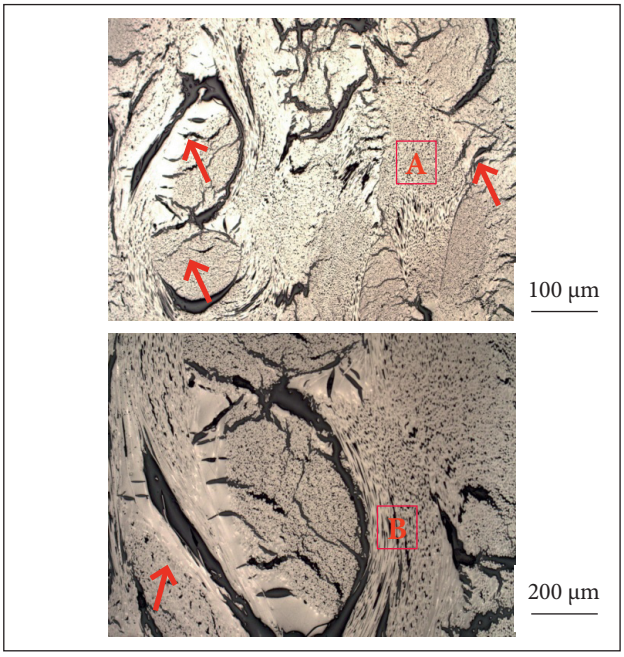

Figure 11. Photomicrographs of the pristine carbon fiber/phenolic resin composite.

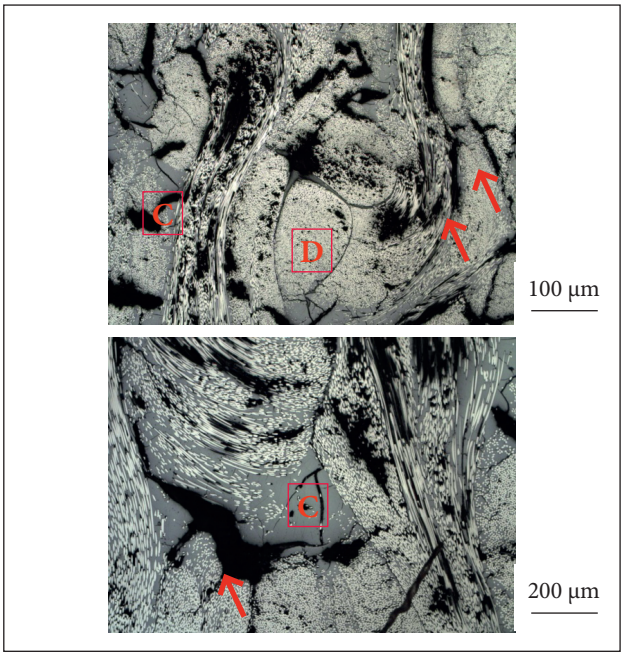

Figure 12. Photomicrographs of the 500 °C treated samples.

As mentioned before, the image analysis for porosity identification was done by using optical microscopy and Image J software. The analysis is shown in Fig. 16. Given a gray scale ranging from 0 (completely black) to 255 (pure white), the threshold level which allowed for isolation of the pores was 28. That is, shades below 28 were converted to black and above the blank value (Von Dollinger *et al.* 2014). Table 4 presents the mean values obtained for each set of specimens.

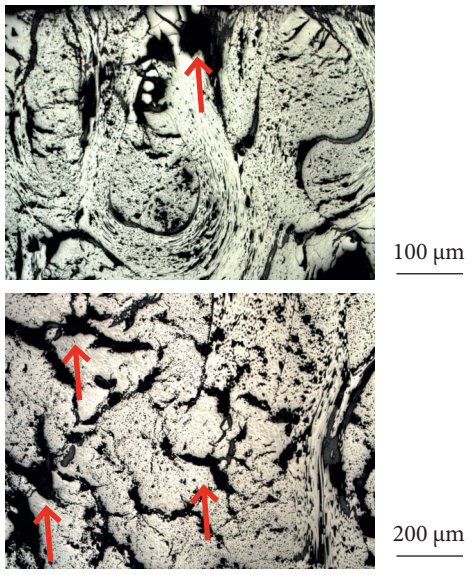

Figure 13. Photomicrographs of the 1,000 °C treated samples.

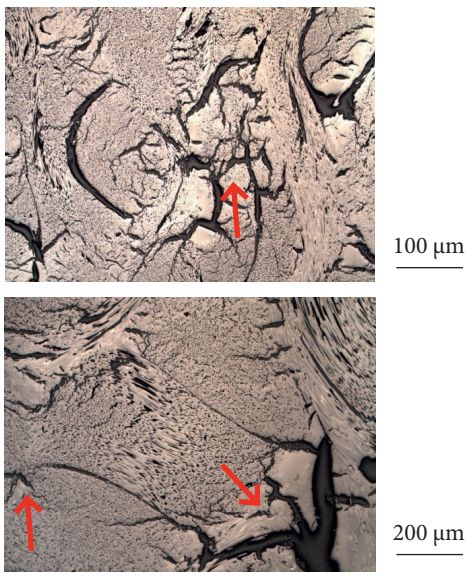

Figure 14. Photomicrographs of the 1,500 °C treated samples.

A slight increase in the percentage porosity is noted in accordance with the treatment temperature caused by the contraction of the composite along with weight loss due to pyrolysis of the phenolic matrix.

Figure 17a shows a microfractograph of the fracture surface of the pristine carbon fiber/phenolic resin composite under shear mode. A high fiber concentration in the direction parallel to the picture plane (position A) is found and a detail of a fiber strand in the perpendicular direction to the picture plane (position B) can also be identified. Figure 17b shows the detail of the fiber strand where a number of "bean shape" carbon fiber cross section can be seen. The bean shape cross section is typical from ex-rayon carbon fibers.

The microfractographs features are not changed with the applied treatment temperatures. The images shown are typical of the material.

Figure 18 shows grid mesh obtained for the exit cone element and the model profile corresponding to the levels

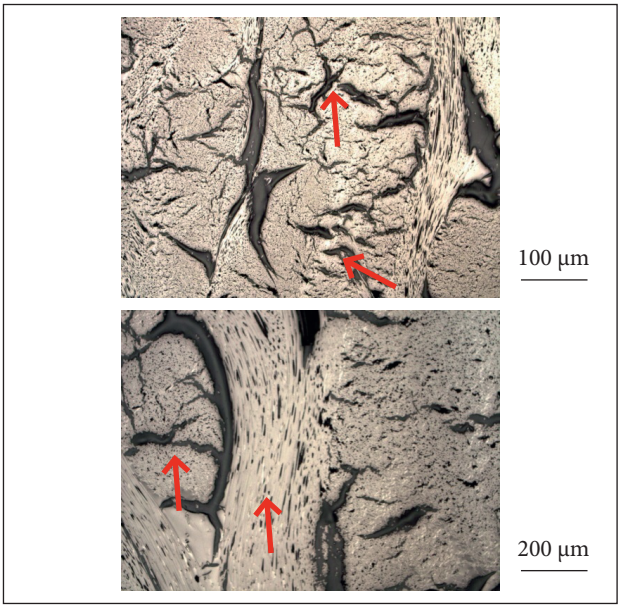

Figure 15. Photomicrographs of the 2,000 °C treated samples.

Table 4. Percentage porosity of the specimens.

Samples	Porosity average (%)
As-molded	21.22 ± 1.62
S500	23.43 ± 3.27
S1000	24.12 ± 2.56
S1500	26.15 ± 1.89
S2000	27.76 ± 2.88

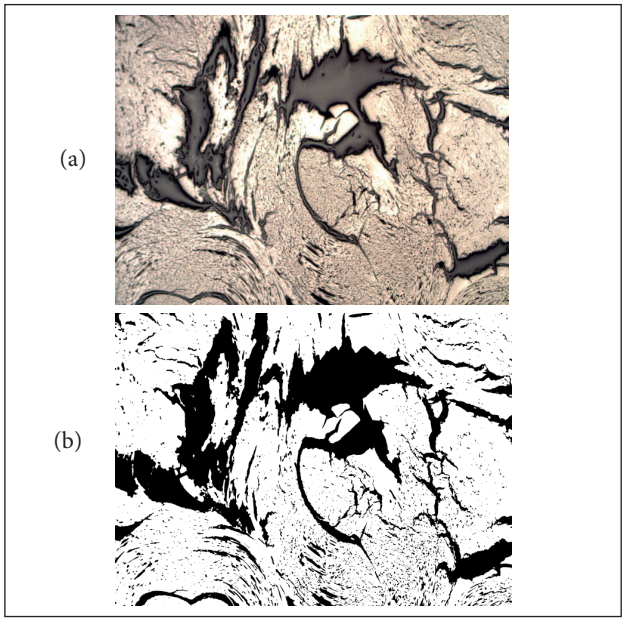

Figure 16. (a) Photomicrograph of a region of the sample; (b) Image from Image J treated area.

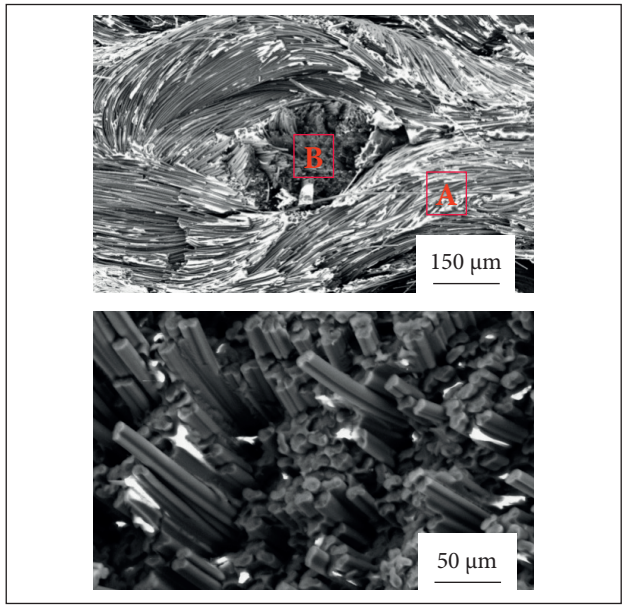

Figure 17. SEM photomicrographs of the untreated samples.

of shear stress. The region of the model in which the shear stress attains its maximum values is the nozzle extension entrance. The ultimate shear stress of 2.35 MPa was calculated taking the most extreme situation of propeller burning operation.

The positive and negative values in the color scale are due to the reversal of the direction of shear stress in relation to the reference which was adopted in the calculation process.

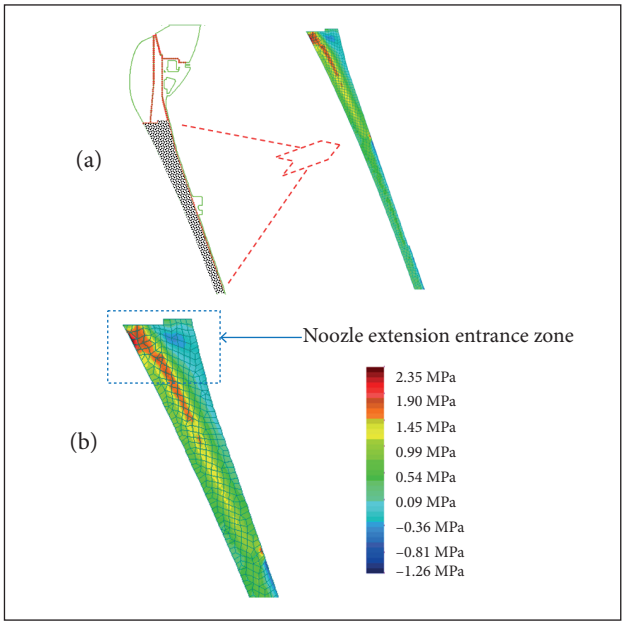

Figure 18. (a) Profile of the nozzle with the correspondent theoretical shear stress level; (b) Color scale referred to stress levels through the nozzle geometry.

CONCLUSION

Carbon fiber/phenolic resin composites were submitted to high temperature heat treatment in order to evaluate the changes in shear behavior. Heat treatment temperatures were 500, 1,000, 1,500 and 2,000 °C. In general, shear strength, measured by the Iosipescu shear mode, reduces as the temperature goes higher, whereas the shear modulus increases.

The microstructure is affected by heat treatment temperatures by the formation of a network of microcracks and pores throughout the material. The void volume percentage of the composite increases as a function of heat treatment temperature due to the weight loss from both the fiber and the resin during the pyrolysis process. These changes in the void volume influence negatively the shear strength.

The shear strength ranged from 22.43 MPa for the pristine carbon fiber/phenolic resin composite to 4.05 MPa for the same composite treated between over 1,000 and up to 2,000 °C. For the shear modulus, obtained values ranged between 1.55 and 3.85 GPa by increasing the heat treatment temperature.

In general, shear tests on composite samples heat treated above 1,000 °C revealed fragile behavior of the tested material due to the formation of carbon matrix, pores and microcracks. Higher shear deformations are observed for composites heat treated at high temperatures (T > 1,500 °C), because

of an incipient formation of oriented crystalline graphitic structures in the carbon matrix.

The shear stress value calculated theoretically (2.35 MPa) corresponds to ~ 58% of the minimum value obtained experimentally in this study (4.05 MPa), *i.e.* it has a 1.72 of safety factor. Therefore, the nozzle extension entrance, as it is currently manufactured, fulfills the design requirements.

REFERENCES

Almeida LEN (2007) Obtenção e caracterização de compósitos ablativos de matrizes fenólica e fenólica modificada com epóxi, com reforço de fibra de carbono picada (Master's thesis). São José dos Campos: Instituto Tecnológico de Aeronáutica.

Barbosa CAL (2004) Obtenção e caracterização de materiais ablativos a base de compósitos de fibra de carbono/resina fenólica (Master's thesis). São José dos Campos: Instituto Tecnológico de Aeronáutica.

Dias FMC (2001) Desenvolvimento de processos de fabricação de estruturas em material compósito ablativo para tubeiras de foguetes (Master's thesis). São José dos Campos: Instituto Tecnológico de Aeronáutica.

Gonçalves A (2008) Caracterização de materiais termoestruturais a base de compósitos reforçados com fibras de carbono (CRFC) e carbono reforçado com fibras de silício (SiC) (PhD thesis). São José dos Campos: Instituto Tecnológico de Aeronáutica.

Hall WB (1988a) Standardization of the carbon-phenolic materials and processes. Vol. 1. Experimental studies. NASA Grant No. NAG8-545.

Hall WB (1988b) Standardization of the carbon-phenolic test methods and specification. Vol. 2. NASA Grant No. NAG8-545.

Machado HA (1990) Análise uni-dimensional para escoamento bifásico e transferência de calor em tubeiras de foguetes a propelente sólido (Undergraduate thesis). Rio de Janeiro: Universidade Federal do Rio de Janeiro.

Martins FR (2014) Caracterização do fresamento de chapas de compósito polímero reforçado com fibras de carbono (PRFC) (PhD thesis). Campinas: Universidade Estadual de Campinas.

Minges ML (1969) Thermal physical characteristics of high-performance ablative composites. J Macromol Sci Chemistry A 3(4):613-639. doi: 10.1080/10601326908053832

Neuse EW (1973) Polymers for potential use as charring ablators under hyperthermal re-entry conditions: a review of recent developments. Mater Sci Eng 11(3):121-150. doi: 10.1016/0025-5416(73)90060-8

Nichols RL, Hall WB (1988a) Standardization of the carbon-phenolic materials and processes. Vol. 1. Experimental studies. NASA Grant No. NAG8-545.

Nichols RL, Hall WB (1988b) Standardization of the carbon-phenolic test methods and specification. Vol. 2. NASA Grant No. NAG8-545.

Palmério AF (2013) Introdução à tecnologia de foguetes.

Pardini LC, Levy Neto F (2006) Compósitos estruturais: ciência e tecnologia. São Paulo: Edgar Blücher.

Ramesh Kumar R, Vinod G, Renjith S, Harikrishnan R (2005) Thermo-structural analysis of composite structures. Mater Sci Eng 412(1):66-70. doi: 10.1016/j.msea.2005.08.065

Savage G (1993) Carbon /carbon composites. London: Chapman & Hall.

Silva SFC (2015) Tecnologia de plasma para estudo das propriedades ablativas em compósitos obtidos por bobinagem para uso aeroespacial (PhD thesis). Campinas: Universidade Estadual de Campinas.

Teixeira HS, Silva HP, Machado HA, Shimote WK (2007) Análise termo-elástica de tubeira do 2º estágio do VLS-1. Código: 590-213100/B0001. Relatório Técnico No. ASE-RT-007.

Thimoteo HPC (1986) Estudo do comportamento ablativo de composições fenólicas com carga (Master's thesis). Rio de Janeiro: Universidade Federal do Rio de Janeiro.

Tick SJ, Huson GR, Griese R (1965) Design of ablative thrust chambers and their materials. J Spacecraft Rockets 2(3):325-331. doi: 10.2514/3.28179

Von Dollinger CFA, Souza WO, Pardini LC (2014) Evaluation of porosity during pyrolysis of carbon fiber/phenolic resin composites. Proceedings of the 2nd Brazilian Conference on Composite Materials (BCCM 2); São José dos Campos, Brazil.

Williams SD, Cury DM (1992) Thermal protection materials. Thermophysical property data. NASA Reference Publication 1289.